International Journal of Theoretical Physics, Vol. 7, No. 3 (1973), pp. 183–197

Internal Instability in a Reissner–Nordström Black Hole

MICHAEL SIMPSON and ROGER PENROSE

Department of Mathematics, Birkbeck College, London

Received: 1 April 1972

Abstract

The question of the effect of asymmetries in gravitational collapse is investigated by considerations of test electromagnetic fields in an extended Reissner–Nordström background. It is found, with the aid of computer calculations, that instabilities in the test field arise at the inner (Cauchy or anti-event) horizon, though not at the outer (event) horizon. Thus it is reasonable to infer that in the full coupled Einstein–Maxwell theory the inner horizon will not survive as a non-singular hypersurface when asymmetric perturbations are present, but will instead become a space-time curvature singularity.

The gravitational collapse of a star which is too massive to form a white dwarf or neutron star presents a now familiar picture. If spherical symmetry is assumed, then collapse through a black hole to a central space-time singularity at which curvatures mount to infinity is implied by general relativity (Penrose, 1969a). It is also known from general theorems (Hawking & Penrose, 1970) that even when spherical symmetry is not assumed, a space-time singularity must nevertheless still arise whenever trapped surfaces occur. However, the nature and location of these singularities is left completely open by the theorems. According to a frequently stated conjecture (Carter, 1971; Israel, 1967, 1968; Hawking, 1972), the external field of the black hole which results from a gravitational collapse should approach that of a Kerr–Newman (Kerr, 1963; Boyer & Lindquist, 1967; Newman *et al.*, 1965) solution of the Einstein–Maxwell equations, characterized by just three parameters: mass m, charge e, and angular momentum a. There is however no reason to believe that the internal field near the (ring) singularity of these solutions should be an accurate representation of the physical space-time resulting from a realistic collapse. Indeed, the presence of closed timelike curves near the singularities (Carter, 1968) would seem to argue against any too close relation between the models and physical reality.

The Kerr–Newman solutions with $m > \sqrt{(a^2 + e^2)} > 0$ possess the

Copyright © 1973 Plenum Publishing Company Limited. No part of this publication may be reproduced, stored in a retrieval system, or transmitted, in any form or by any means, electronic, mechanical, photocopying, microfilming, recording or otherwise, without written permission of Plenum Publishing Company Limited.

characteristic feature that there is not only an outer (absolute) event horizon (surface of the black hole) but also an inner horizon (the anti-event horizon) (Penrose, 1969b) which is a Cauchy horizon (Hawking, 1966, 1967) for any appropriate initial data hypersurface used to set up the problem. Our contention in this note is that if the initial data is generically perturbed then the Cauchy horizon does not survive as a non-singular hypersurface. It is strongly implied that instead, genuine space-time singularities will appear along the region which would otherwise have been the Cauchy horizon.

We consider here only a special case, namely that when the angular momentum is zero, but mass and charge parameters m and e are both present (with $m > |e|$). We add an electromagnetic test field as a perturbation and show (by computer calculation) that singularities in the electromagnetic field occur at the Cauchy horizon. It is reasonable to infer that when the gravitational–electromagnetic coupling is added, then the Cauchy horizon would degenerate into a curvature singularity.

Our unperturbed space-time can be described by the Reissner–Nordström metric, given in the form†

$$(1 - 2m/r + e^2/r^2)\,dt^2 - (1 - 2m/r + e^2/r^2)^{-1}\,dr^2 - r^2(d\theta^2 + \sin^2\theta\, d\phi^2) \tag{1}$$

where r, t, θ, ϕ are the radial, time, and two angular coordinates respectively. The coordinate singularities due to the distinct zeros $r_+, r_- (r_+ > r_-)$ of $(1 - 2m/r + e^2/r^2)$, corresponding to the event horizon and Cauchy horizon respectively, divide the manifold covered by this coordinate system into the three regions $r > r_+$, $r_- < r < r_+$ and $r < r_-$. Each of these can be parametrised by the retarded and advanced null coordinates u, v given by

$$u = \begin{cases} t - f(r), & r > r_+ \text{ and } r < r_- \\ t + f(r), & r_- < r < r_+ \end{cases}$$
$$v = \begin{cases} t + f(r), & r > r_+ \text{ and } r < r_- \\ -t + f(r), & r_- < r < r_+ \end{cases} \tag{2}$$

where $f(r) = \int (1 - 2m/r + e^2/r^2)^{-1}\,dr$ and u, v have range $(-\infty, \infty)$ in each of the three regions. The parts of the manifold can be represented by the 'blocks' of Fig. 1 for constant values of the angular coordinates. The edges of the blocks are identified as indicated. To the three regions A, B, C there correspond further regions A', B', C' obtained by applying the transformation $u \to -u$, $v \to -v$ which reverses the light cone structure. A maximal analytic extension‡ of the Reissner–Nordström solution may then

† See, for example, C. Møller (1952). *The Theory of Relativity*. Clarendon Press, Oxford.

‡ This procedure is due to J. C. Graves and D. R. Brill (1960). *Physical Review*, **120**, 1507.

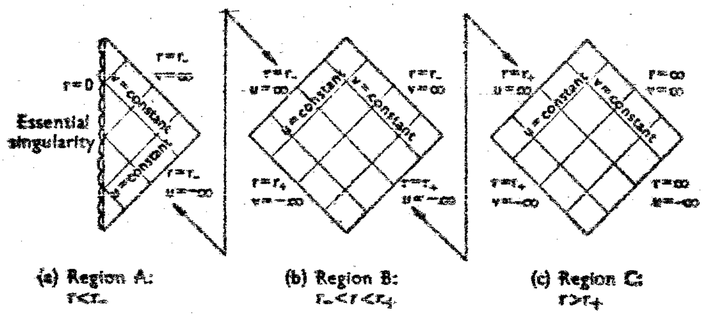

Figure 1.

be constructed by piecing together copies of the six blocks in an analytic fashion so that each overlapping edge is covered by either a (u,r) or (v,r) system of coordinates (with the exception of the corners of each block). The resulting 'ladder' shown in Fig. 2 is infinitely extendible in both directions.

In this space-time the edge of a freely collapsing body is represented by a future-directed timelike geodesic which passes from the exterior region C through B to the interior region A. The nature of the analytic extension allows us to contemplate the possibility (Penrose, 1968) of an observer following in the wake of the collapsing body from C to B, then avoiding

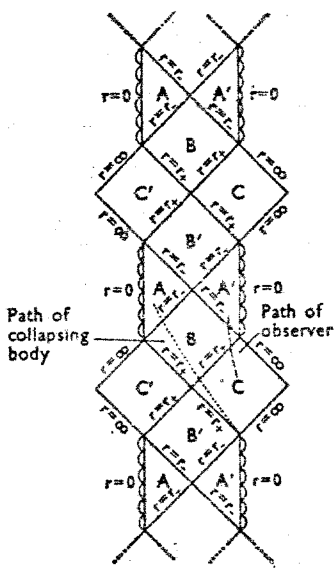

Figure 2.

region A by pursuing instead a (necessarily) non-geodesic trajectory through $r = r_-$ into region A', whose history is not determined by data specified in C. The observer is not however assured of a smooth passage over the Cauchy horizon $r = r_-$ between B and A'. In the instant before crossing he is in a position to observe the entire history of region C and it may be that in consequence of receiving the full (back-scattered) effects of the outgoing radiation field from C he will encounter unbounded curvatures in the vicinity of $r = r_-$. If arbitrary smooth initial data for our electromagnetic test field given on a spacelike hypersurface in C fail to determine limiting values as $r = r_-$ is approached, things look bad for our observer. If such limits are forthcoming, he appears to have chances of getting

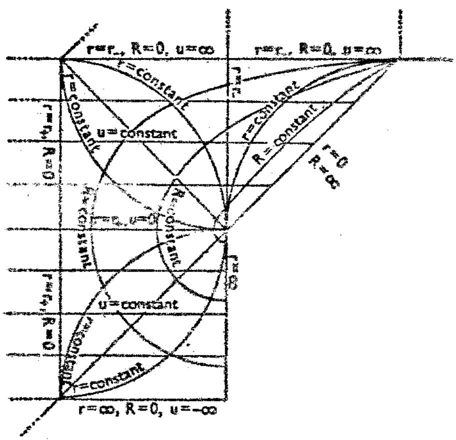

Figure 3.

through. We proceed to set up the necessary apparatus for making such an investigation.

After first performing the conformal transformation $ds \to r^{-1} ds$ we further transform the metric, leaving the angular coordinates unchanged and defining new coordinates u' and R by

$$u' = \begin{cases} -e^{-Au}, & r_+ \leqslant r < \infty \\ e^{Au}, & 0 < r \leqslant r_+ \end{cases}$$

$$R = \frac{r_+ - r}{Au' r r_+}, \qquad 0 \leqslant r < \infty \qquad \text{where } A = \frac{r_+ - r_-}{2r_+^2} \tag{3}$$

These coordinates cover the three regions C, B, and A'. The outgoing null directions are given by $u' = \text{constant}$, while R is an affine parameter along those directions, i.e. $\nabla^a u' \nabla_a R = 1$. Dropping the prime on u, Fig. 3 shows the disposition of the coordinate curves. The metric is now given by

$$ds^2 = g(u, R)\, du^2 + 2\, du\, dR - (d\theta^2 + \sin^2\theta\, d\phi^2) \tag{4}$$

where

$$g(u,R) = R^2\{(3\alpha-2) + \tfrac{1}{2}(1-\alpha)(3\alpha-1)uR + \tfrac{1}{4}\alpha(1-\alpha)^2u^2R^2\}$$

and

$$\alpha = \frac{r_-}{r_+}, \qquad 0 \leqslant \alpha < 1$$

$\alpha = 0$ gives the Schwarzschild limiting case.

Seeking to employ the Newman–Penrose spin coefficient formalism (Newman & Penrose, 1962) we put $l^a = \nabla^a u$, tangent to the outgoing null hypersurfaces, and define three other vectors n^a, m^a, $\bar{m}^a$ to complete a null tetrad satisfying the conditions that n^a shall be a real future-pointing null vector lying in the plane spanned by $\nabla^a u$ and $\nabla^a R$, m^a and its conjugate $\bar{m}^a$ shall be complex null vectors, and $l_a n^a = -m_a \bar{m}^a = 1$, $l_a m^a = n_a m^a = 0$. We take

$$\begin{aligned} n^a &= \nabla^a R + \tfrac{1}{2}g(u,R)\nabla^a u \\ m^a &= \frac{1}{\sqrt{2}}(\nabla^a \theta + i\sin\theta\nabla^a\phi) \end{aligned} \tag{5}$$

Using this tetrad, nine of the twelve spin coefficients are zero, the exceptions being

$$\begin{aligned} \alpha &= \tfrac{1}{2}(n^a\bar{m}^b\nabla_b l_a - \bar{m}^a\bar{m}^b\nabla_b m_a) = -\frac{\cot\theta}{2\sqrt{2}} \\ \beta &= \tfrac{1}{2}(n^a m^b\nabla_b l_a - \bar{m}^a m^b\nabla_b m_a) = \frac{\cot\theta}{2\sqrt{2}} \\ \gamma &= \tfrac{1}{2}(n^a n^b\nabla_b l_a - \bar{m}^a n^b\nabla_b m_a) = \frac{1}{4}\frac{\partial g}{\partial r} \end{aligned} \tag{6}$$

where $g(u,R)$ is given by (4).

Defining the three complex components of the electromagnetic field tensor F_{ab} by

$$\begin{aligned} \phi_0 &= F_{ab}l^a m^b \\ \phi_1 &= \tfrac{1}{2}F_{ab}(l^a n^b - \bar{m}^a m^b) \\ \phi_2 &= F_{ab}\bar{m}^a n^b \end{aligned} \tag{7}$$

and writing $D = l^a\nabla_a$, $\Delta = n^a\nabla_a$, $\delta = m^a\nabla_a$, the spin coefficient form of Maxwell's equations is

$$\begin{aligned} D\phi_1 - \delta\phi_0 &= -2\alpha\phi_0 \\ D\phi_2 - \delta\phi_1 &= 0 \\ \delta\phi_1 - \Delta\phi_0 &= -2\gamma\phi_0 \\ \delta\phi_2 - \Delta\phi_1 &= -2\beta\phi_2 \end{aligned} \tag{8}$$

We next introduce (Penrose, 1967; Newman & Penrose, 1968) the angular differential operator ð. A quantity η is said to have spin weight s if under a transformation $m^a \to e^{i\chi} m^a$ it transforms as $\eta \to e^{is\chi}\eta$. It is readily seen from (7) that ϕ_0, ϕ_1, ϕ_2 have spin weights 1, 0 and −1 respectively; ð is then defined for a quantity η of spin weight s by the equation

$$ð\eta = -(\sin\theta)^s \left\{\frac{\partial}{\partial\theta} + \frac{i}{\sin\theta}\frac{\partial}{\partial\phi}\right\}\{(\sin\theta)^{-s}\eta\} \tag{9}$$

The operator $\bar{ð}$ is similarly defined:

$$\bar{ð}\eta = -(\sin\theta)^{-s} \left\{\frac{\partial}{\partial\theta} - \frac{i}{\sin\theta}\frac{\partial}{\partial\phi}\right\}\{(\sin\theta)^{s}\eta\} \tag{10}$$

(9) and (10) reduce to

$$\begin{aligned} ð\eta &= -\sqrt{2}\,\delta\eta + s\eta\cot\theta \\ \bar{ð}\eta &= -\sqrt{2}\,\bar{\delta}\eta - s\eta\cot\theta \end{aligned} \tag{11}$$

Substituting ϕ_0, ϕ_1, ϕ_2 in turn for η in (11) and putting s equal to the corresponding spin weight, we see that Maxwell's equations (8) may be put in the form

$$\begin{aligned} D\phi_1 + \frac{1}{\sqrt{2}}\bar{ð}\phi_0 &= 0 \\ D\phi_2 + \frac{1}{\sqrt{2}}\bar{ð}\phi_1 &= 0 \\ (\Delta - 2\gamma)\,\phi_0 + \frac{1}{\sqrt{2}}ð\phi_1 &= 0 \\ \Delta\phi_1 + \frac{1}{\sqrt{2}}ð\phi_2 &= 0 \end{aligned} \tag{12}$$

We define the quantities

$$H_m = \int {}_1\bar{Y}_{1,m}\,\phi_0\,d\theta\sin\theta\,d\phi, \qquad m = -1, 0, 1 \tag{13}$$

where ${}_1Y_{1,m}$ is a spin s spherical harmonic given by substituting for s and l in the defining equations

$$\begin{aligned} {}_sY_{l,m} &= \begin{cases} \left[\dfrac{(l-s)!}{(l+s)!}\right]^{1/2} ð^s Y_{l,m}, & 0 \leqslant s \leqslant l \\ (-1)^s \left[\dfrac{(l+s)!}{(l-s)!}\right]^{1/2} \bar{ð}^{-s} Y_{l,m}, & -l \leqslant s \leqslant 0 \end{cases} \\ {}_s\bar{Y}_{l,m} &= (-1)^{m-s}\,{}_{-s}Y_{l,-m} \end{aligned} \tag{14}$$

where $l=0, 1, \ldots$; $m=-l, \ldots, l$; and $Y_{l,m}$ are the ordinary spherical harmonics. We note the property that if p is a quantity of spin weight $l+1$ then

$$\int {}_sY_{l,m}\bar{\eth}^{l-s+1} p\, d\theta \sin\theta\, d\phi = 0 \tag{15}$$

Dropping the subscript from H and using (11), (12) and (15), together with the three commutator relations for scalars ϕ

$$\begin{aligned}(\Delta D - D\Delta)\phi &= 2\gamma D\phi \\ (\delta D - D\delta)\phi &= 0 \\ (\bar{\eth}\eth - \eth\bar{\eth})\phi &= 2s\phi\end{aligned} \tag{16}$$

where in the last equation ϕ is considered to be of spin weight s, we derive a linear homogeneous second-order partial differential equation in H of hyperbolic type:

$$\mathscr{L}[H] = \{(\Delta - 4\gamma)D + (1 - 2D\gamma)\}H = 0 \tag{17}$$

Substituting for Δ, D, γ, we have

$$\mathscr{L}[H] = \left\{\frac{\partial^2}{\partial u\,\partial R} - \frac{g}{2}\frac{\partial^2}{\partial R^2} - \frac{\partial g}{\partial R}\frac{\partial}{\partial R} + \left(1 - \frac{1}{2}\frac{\partial^2 g}{\partial R^2}\right)\right\}H = 0 \tag{18}$$

or

$$\frac{\partial^2 H}{\partial u\,\partial R} - \frac{1}{2}\frac{\partial^2}{\partial R^2}(gH) + H = 0$$

where $g(u, R)$ is given by (4).

The canonical form of (18),

$$\left\{\frac{\partial^2}{\partial u\,\partial v} + A(u,v)\frac{\partial}{\partial v} + B(u,v)\right\}H = 0$$

requires for its explicit description the inverse (for R) of the transformation

$$v = \frac{R\exp\left[\dfrac{2(1-\alpha)}{2+(1-\alpha)uR}\right]}{(2-\alpha uR)^{\alpha^2}(2+(1-\alpha)uR)^{(1-\alpha^2)}} \tag{19}$$

which is not forthcoming. Nor does Riemann's method of solution of the initial value problem for partial differential equations of hyperbolic type assist us since the adjoint equation to (18)

$$\mathscr{L}^*[J] = \frac{\partial^2 J}{\partial u\,\partial R} - \tfrac{1}{2}g\frac{\partial^2 J}{\partial R^2} + J = 0 \tag{20}$$

is related to (18) by

$$\frac{\partial^2}{\partial R^2}\mathscr{L}^*[X] = \mathscr{L}\left[\frac{\partial^2 X}{\partial R^2}\right] \tag{21}$$

i.e. if $J = X$ is a solution of $\mathscr{L}^*[J] = 0$ then $H = \partial^2 X/\partial R^2$ is a solution of $\mathscr{L}[H] = 0$. Finding exact solutions of (20), which must be achieved in order to construct a Green's function, is consequently equivalent to finding them for (18), and excepting one trivial case no exact solutions of either have been found.

We note that at $r = \infty$, given by $uR = 2/(\alpha - 1)$ in our present coordinate system, $1 - \frac{1}{2}\partial^2 g/\partial R^2 = 0$ and hence (18) reduces to

$$\left\{\frac{d}{du} + R(1-\alpha)\right\} DH = 0$$

giving

$$\frac{d}{du}(R^2 \, DH) = 0 \tag{22}$$

Thus from (13) we have the integral conservation law

$$\frac{d}{du}\int {}_1Y_{1,m} R^2 \, D\phi_0 \, d\theta \sin\theta \, d\phi = 0 \tag{23}$$

the integration being carried out over the sphere at infinity. This integral is one of the Newman–Penrose absolutely conserved quantities (Penrose, 1967; Newman & Penrose, 1968).

In the apparent absence of explicit analytic solutions of (18) numerical solutions have been sought by the usual method for hyperbolic partial differential equations (Smith, 1969). The characteristic directions (null lines) are given by

$$\begin{aligned} du &= 0 \\ \frac{dR}{du} + \tfrac{1}{2}g(u, R) &= 0 \end{aligned} \tag{24}$$

and putting

$$p = \frac{\partial H}{\partial u}, \qquad q = \frac{\partial H}{\partial R} \qquad \text{and} \qquad f(u, R, q, H) = q\frac{\partial g}{\partial R} + H\left(\frac{1}{2}\frac{\partial^2 g}{\partial R^2} - 1\right)$$

the differential relationships

$$\begin{aligned} dp &= \tfrac{1}{2}g \, dq + f \, dR \\ dq &= f \, du \end{aligned} \tag{25}$$

represent (18) along the respective characteristics. We also have along $du = 0$,

$$dH = q \, dR \tag{26}$$

Successive approximations to H, p, q at any point X of the characteristic grid in terms of their values at immediately preceding grid points on the characteristics through X are obtained by iterative use of the finite difference equivalents of (25) and (26). If values of p are not required the first equation in (25) becomes redundant since p appears neither in the second of (25) nor in (26).

The solution of the second equation in (24) is given by (19). The R-coordinate of a point on the characteristic grid given by specified values of u, v could therefore be found using Newton's method to solve (19) to any desired accuracy, but this is a lengthy procedure to undertake for every point of the grid and is consequently employed only at points on the initial hypersurface. Elsewhere a Runge–Kutta approximation† using (24) gives the values of R at successive grid points on each v-characteristic. When $u = 0$ (19) becomes $v/R = \text{constant}$, and by scaling v so that this constant is unity we obtain a direct check on the accuracy of the approximation for R in the region $u \leqslant 0$.

Initial values of H, q are specified on a pair of null lines $u = u_0$, $v = v_0$ ($u_0 < 0$, $v_0 \geqslant 0$), the initial value of p if required being then uniquely determined on these characteristics. For the computation‡ it is necessary to choose a numerical value for the ratio $\alpha = r_-/r_+$ and we put $\alpha = \frac{3}{4}$, for which the maximum divergence of the v-characteristics occurs on $u = 0$. Along $v = \text{constant}$, dR/du has a maximum and minimum of order v^2 on either side of $u = 0$. The number of grid points required to furnish a reasonably accurate solution therefore rises sharply as v increases placing practical limits on the extent of the solution domain in this direction. Within these bounds results of interest have been obtained.

Several functions have been used as initial data. In particular setting $v_0 = 0$ and choosing H, p, q to be zero on $v = v_0$, the C^1 initial function

$$H_0 = \begin{cases} K^2(a-R)^2, & 0 \leqslant R \leqslant a \\ 0, & a \leqslant R \leqslant \dfrac{2}{(\alpha-1)u_0} \end{cases} \tag{27}$$

for $u = u_0$ has been tried with various values of u_0 and a. Profiles along $u = \text{constant}$ of the solution obtained, from (27) with $u_0 = -100$ and $a = 0{\cdot}0525$ are shown in Fig. 5 while cross-sections along $v = \text{constant}$ are displayed in Fig. 6. Figure 4 shows the relative disposition of the u- and v-characteristics employed, drawn to the same scale. These graphs show features typical of all the numerical solutions investigated.

By choosing the initial value of DH on the boundary to be zero we are assured by (22) of its remaining zero all the way up $r = \infty$. Graphs of H for any constant negative value of u are asymptotically flat in consequence. As u increases from -100 to 0 the number of oscillations of the solution for $u = \text{constant}$ goes up, remaining finite for any particular $u < 0$. On $u = 0$ we apparently have an unbounded number of well-damped oscillations, and as we enter the region $u > 0$ the amplitude of these oscillations rises sharply and they appear to diverge more and more violently as u

† See, for example, P. K. Henrici (1968). *Discrete Variable Methods in Ordinary Differential Equations*. Wiley, New York.

‡ All programs were run on the University of London's Atlas computer.

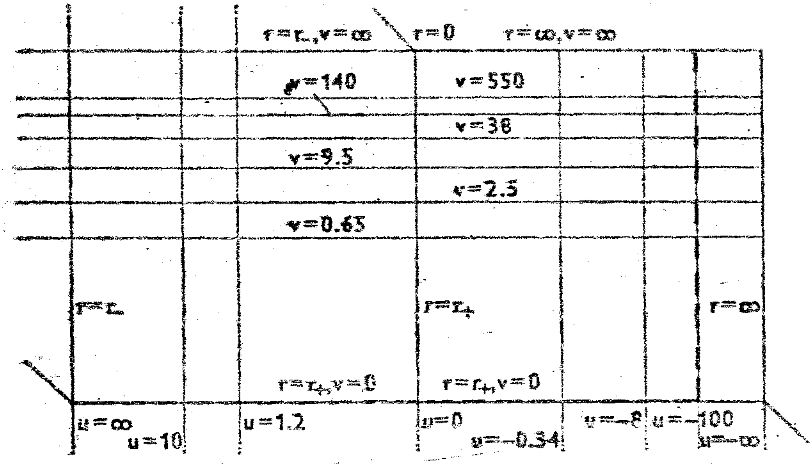

Figure 4.

further increases. It can be seen in graphs (e) and (f) of Fig. 5 that these unstable oscillations are situated 'very close' to the Cauchy horizon $r = r_-$ in terms of the affine parameter R.

The solution for v = constant to the left of any neighbourhood of $u = 0$ appears to settle down rapidly as v is increased while the number of oscillations of decreasing amplitude near $u = 0$ continues to rise. It seems reasonable to extrapolate from this to the picture at $v = \infty$ for $u < 0$ featuring an

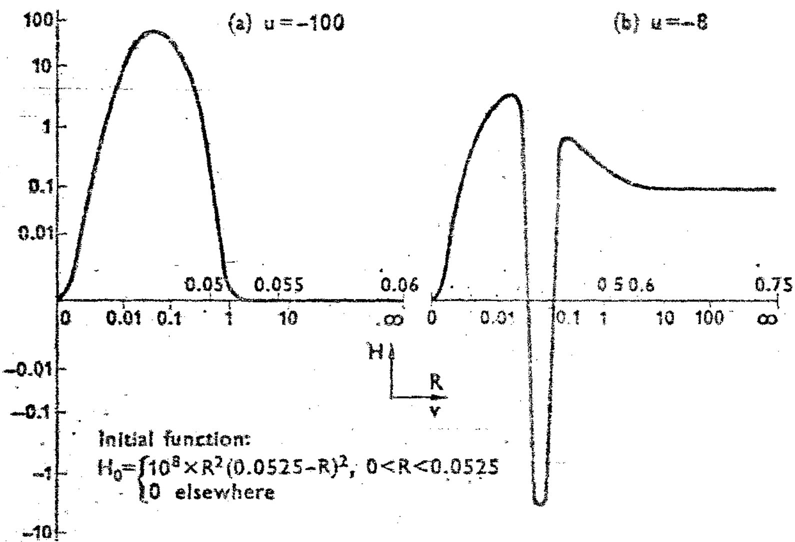

Figure 5a, b.

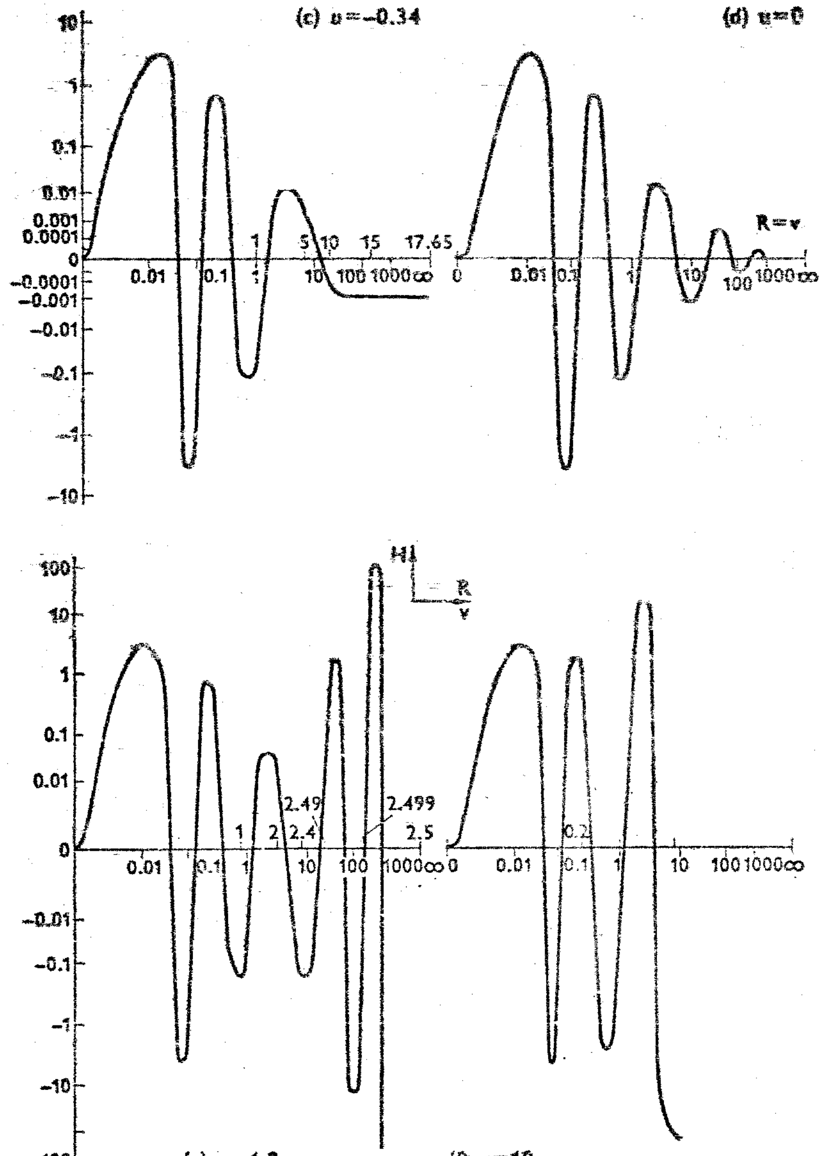

Figure 5c, d, e, f.

infinite number of oscillations, the amplitude of these tending to zero as $u \to 0$. For $u > 0$ however the solution curve waggles, showing no sign of tending to any limit as v rises.

The numerical procedure is a stable one, alterations of the step lengths in either direction producing no significant deviation from the graphs shown. The numerical evidence therefore points to a singularity in the test field along $r = r_-$ despite the fact that the solution appears to have the limiting value zero as $u \to 0$ and $v \to \infty$ along any curve for which $u \leqslant 0$.

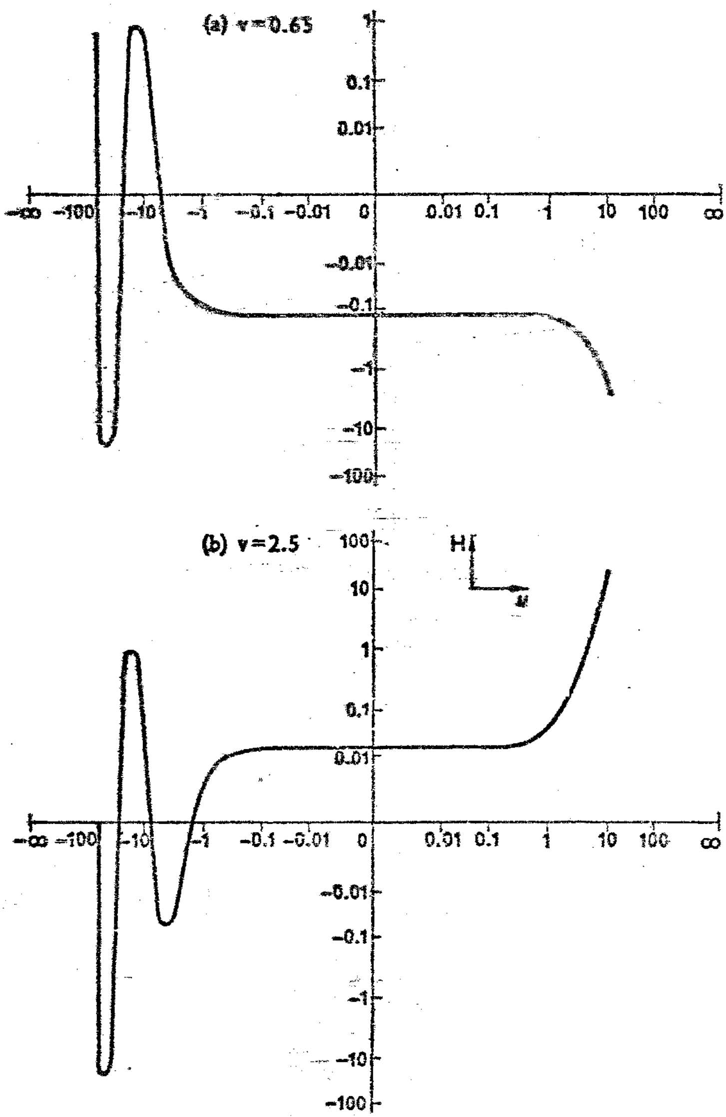

Figure 6a, b.

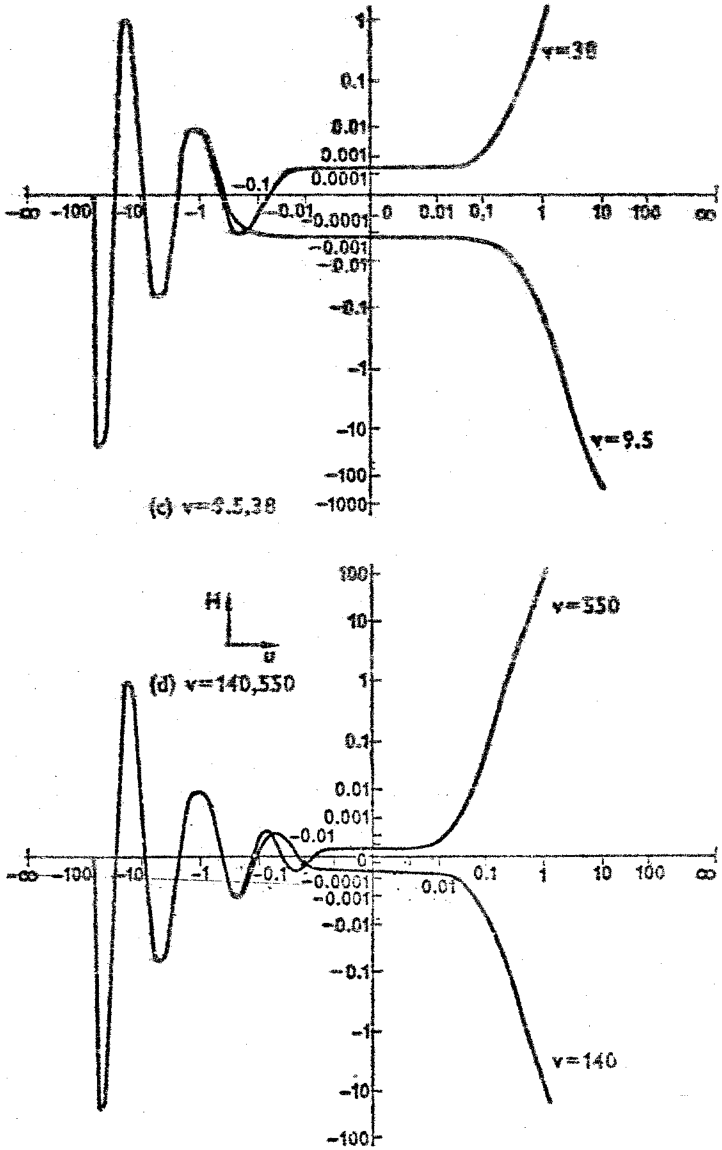

Figure 6c, d.

It is to be expected from analytical considerations of the characteristic initial value problem that the specification of unrestricted null characteristic data will in general produce a shock-wave up the initial hypersurface along which the field equations are violated, i.e. a sheet of charge. This will be so unless subsidiary conditions are imposed (namely the vanishing of certain integrals along the generators of the initial characteristic surface) in order to ensure that the sheet of charge is absent (the shock-wave cannot be directly ascertained from the numerical solution; the apparent initial severity of the graphs in Fig. 6 is partly due to the scale employed).

It is not to be expected that the presence of such a shock-wave should affect our conclusions, since it is only the effect of back-scattering from the wave which enters the region $u > 0$ in which we are mainly interested. However, to make sure of this we ran programs with suitable alternative initial data. In the first instance the effect of such a shock-wave can be substantially lessened and possibly even removed by balancing the initial 'hump' with another of equal size and opposite sign placed further up the hypersurface. The shock-wave can presumably be further reduced by separating two such positive humps with a larger negative hump so that a balance is again achieved (in the first case $\int_{v=v_0}^{v=\infty} H_0\, dR = 0$; in the second $\int_{v=v_0}^{v=\infty} H_0\, dR = \int_{v=v_0}^{v=\infty} [\partial H/\partial u]_{u=u_0}\, dR = 0$). It can also be removed from $u = u_0$ altogether by specifying non-zero data only along $v = v_0$ $(u < 0)$. The shock-wave then resides further along the hypersurface $v = v_0$. There is no reason to believe that the presence of this shock-wave should affect the field at $v = \infty$, $0 \leqslant u < \infty$.

Neither in these cases nor in any others considered has there been any major qualitative difference from the results displayed here. Each set of initial data produces a markedly stable solution while $u \leqslant 0$ followed by immediate signs of instability on crossing into $u > 0$. It therefore seems likely that the field singularity is a property of the partial differential equation (18) rather than any particular initial function and will consequently occur for generic cases of the latter.

It should be pointed out that the situation we consider of placing a *test* solution of Maxwell's equations on a background space-time which satisfies the Einstein–Maxwell equations is not equivalent to considering a small (electromagnetic) perturbation of the Einstein–Maxwell equations. This is because cross-terms arise in the contribution of the Maxwell field to the background space-time via the energy-momentum tensor, producing changes in the background metric of the same order as that of the initial perturbation.† A full treatment of such a perturbation would lead to far more complex equations than those treated here, but we do not believe that the results would be substantially affected. A perturbation analysis cannot in any case give a definitive answer to the problem we consider, since the non-linear effects would ultimately have to be brought in.

From this connection of inferences we conclude that the projected journey of our hypothetical observer through $r = r_-$ looks liable to prove a dangerous undertaking, for the likelihood is that the Cauchy horizon is unstable and that unbounded curvatures will be met in its immediate neighbourhood as soon as the coupling effect of the field back on the space-time is taken into account.

† We are grateful to Dr. R. Wald for pointing this out to us.

References

Boyer, R. H. and Lindquist, R. W. (1967). *Journal of Mathematical Physics*, **8**, 265.
Carter, B. (1968). *Physical Review*, **174**, 1559.
Carter, B. (1971). *Physical Review Letters*, **26**, 331.
Hawking, S. W. (1966). *Proceedings of the Royal Society, A*, **294**, 511; (1967) **300**, 187.
Hawking, S. W. (1972). *Communications in Mathematical Physics*, **25**, 152.
Hawking, S. W. and Penrose, R. (1970). *Proceedings of the Royal Society, A*, **314**, 529.
Israel, W. (1967). *Physical Review*, **164**, 1776.
Israel, W. (1968). *Communications in Mathematical Physics*, **8**, 245.
Kerr, R. P. (1963). *Physical Review Letters*, **11**, 237.
Newman, E. T., Couch, E., Chinnapared, K., Exton, A., Prakash, A. and Torrence, R. (1965). *Journal of Mathematical Physics*, **6**, 918.
Newman, E. T. and Penrose, R. (1962). *Journal of Mathematical Physics*, **3**, 566.
Newman, E. T. and Penrose, R. (1968). *Proceedings of the Royal Society, A*, **305**, 175.
Penrose, R. (1967). 'An Analysis of the Structure of Space-Time' (Adams Prize Essay, Cambridge). Princeton.
Penrose, R. (1968). 'Structure of Space-Time', in *Battelle Recontres* (Ed. C. M. De Witt and J. A. Wheeler). Benjamin, New York.
Penrose, R. (1969a). *Rivista del nuovo cimento*, Serie 1, **1**, Numero Speciale, 252.
Penrose, R. (1969b). *Contemporary Physics*, **1**, 545 (International Atomic Energy Agency, Vienna.
Smith, G. D. (1969). *Numerical Solution of Partial Differential Equations*. Oxford University Press.